Testing of bicycle helmets for preadolescents

Corina Klug, Florian Feist, Ernst Tomasch

Abstract This study aims to provide guidelines for a helmet testing procedure especially designed for preadolescents which also takes incorrect use (misuse) into consideration. Based on recommendations from literature, helmets were first tested using a headform with flexible skin, and an add-on mass/inertia to account for the neck. Tests were performed at 6.5 m/s against a 30 degree anvil, both frontally and laterally, in an ideal and a real positioning (misuse) of the helmet. Second, a validated numerical model of one of the tested helmets was established. A parameter study was performed to expand the data of the experimental study. Experiments and simulations were evaluated by applying eleven head injury criteria and, if available, by considering the underlying injury risk curves. Selected tests were also evaluated with the THUMS v4.0 5th percentile female (AF05) head.

The study shows that the approach to adjust mass and inertia of the impactor such to replicate the effect of the neck in oblique impact seems feasible. The study once again indicates the importance of friction: Therefore, the headform's skin should replicate frictional properties very well. The numerical study proved that the impact against a 30 degree anvil is a reasonable choice, maximising almost all criteria. Numerical and experimental studies show that misuse has no detrimental effect on impact protection performance.

Keywords bicycle helmet testing, head injury criteria, preadolescents, FE helmet model

I. INTRODUCTION

In Austria, roughly 480 [1] cyclists aged 10 to 14 years are injured in traffic accidents annually (mean value for 2007-2011), which means 12 out of 1000 children of this age group [2]. This is the highest relative frequency among all age groups. 6 out of 8 patients with diffuse axonal injuries after a bicycle crash with a motor vehicle are younger than 16 [3]. The use of bicycle helmets in Austria is obligatory for children younger than 12 years. Young cyclists very frequently fail to wear their helmets properly [4], which might adversely influence the helmet's effectivity [5],[6].

In Europe, bicycle helmets are tested according to EN 1078: The shock absorption capability of the helmet is determined by propelling a helmet fitted to a rigid headform (specified in EN 960) at 5.4 m/s against a flat, horizontal anvil, or at 4.57 m/s against a kerbstone. The peak acceleration is the only criterion for passing the shock absorption test (threshold: 250 g). In American Standards (16 CFR Part 1203 and SNELL B-95), a hemispherical anvil is used additionally. Internationally, impact velocities and peak acceleration criteria range from 4.5 to 6.3 m/s and 150 (CSA-D113.2-M) to 300 g, respectively. The Australian Standard AS/NZS 2063:2008 additionally defines that 200 and 150 g must not exceed a cumulative duration of 3 and 6 ms, respectively. Consumer information tests apply more stringent criteria, but boundary conditions are almost identical (higher impact velocity up to 6.2 m/s). The current test method was criticized in various studies and alternatives were proposed [7–11]. Major points of criticism are missing tangential velocities, the pure evaluation of peak acceleration without time and rotational loads, the rigid headform and missing friction, i.e. undefined surface properties of the anvil.

Based on multibody simulations [12],[13], recent studies showed that mean resultant impact velocities of the head in traffic accidents and falls is higher than the tested velocity (6.8±2.7 for traffic accidents [12],6.9±1.2 m/s for skidding falls and 6.4±1,2 m/s for curb hitting [13]). Similar tangential velocities and impact angles, respectively, were found in falls and traffic accidents (33±20 deg in traffic accidents [12] and 33.5±8.7 deg in skidding falls and 36±7.7 deg for curb hitting). Further, studies have revealed that a large portion of impact points is not covered by the test area specified in EN 1078. [11]

Dr. F. Feist (phone: +43 316 873 30312, email: florian.feist@tugraz.at) is Senior Scientist, C. Klug is PhD student, and Dr. E. Tomasch is Senior Scientist at the Vehicle Safety Institute at Graz University of Technology, Austria.

More advanced head injury criteria are available: The Head Injury Criterion (HIC) [14] is frequently used in safety regulations. Exposure time and resultant translational acceleration are considered. Several studies highlight the importance of rotational loads on brain injuries [15–19]. Attempts to consider these led to criteria like the Generalized Acceleration Model for Brain Injury Tolerance (GAMBIT) [20] and the Head Impact Power (HIP) [21]. These criteria, however, are rarely used and are not applied in legislative or consumer information testing, since their correlation with real-world injury risk has not yet been entirely proved [16],[22].

The Kleiven criterion (KLC) [19] is a linear combination of HIC and the change of rotational velocity. Direction-dependent scaling factors for the HIP lead to the Power Index (PI), which is a criterion for subdural haematoma (SDH) [23].

Power Rotational Head Injury Criterion (PRHIC) and the Rotational Injury Criterion (RIC) were developed to predict mild TBI considering only rotational loads [24]. In 2011 the Brain Injury Criterion (BRIC), was introduced [25] and later, in 2013 [26], revised and abbreviated as BrIC. The 'new' BrIC is a function of the rotational velocity and was developed for the prediction of brain injuries from AIS 1 to AIS 6 [26]. It was found to correlate with the response of the simulated injury monitor (SIMon) and the Global Human Body Models Consortium (GHMBC) head model [26].

In finite element (FE) models, the Cumulative Strain Damage Measure (CSDM) is frequently applied as an injury criteria [24],[26],[27]. It is a measure for the percentage of the brain's volume that exceeds a pre-defined strain.

This current study funded by the Austrian Ministry for Transport, Innovation and Technology (bmvit) shall provide guidelines for a future helmet testing procedure tailored to preadolescents, also considering oblique impact and misuse.

II. METHODS

Habitual and Impact Study

To determine real-world wearing habits, a survey on (mis)use, comfort and personal perception was conducted among 147 children aged 3 to 14 years. The distance between eyebrow and helmet leading edge, as well as the slack in the chin strap were established. Further, it was recorded whether the helmet was worn straight with properly adjusted chin straps.

Experimental Study

An enhanced helmet-testing concept was established based on literature reviews, habitual and video study (impact kinematics were analysed by carrying out video analysis of bicycle crashes on internet video portals).

Literature indicated that:

- the resultant impact velocity should be increased to 6.5 m/s [12],[13],
- the impact angle should lie between 30 and 60 degree to get appropriate tangential velocities [12],[13],
- the anvil should be covered with 80 grain abrasive paper, which provides a coefficient of friction of 0.5 as used in ECE R - 22.05 [28],
- the headform should be equipped with a flexible skin [29], and
- the headform's mass and inertia needed to be increased in order to replicate the influence of upper body and neck [30].

The habitual study indicated two typical types of misuse:

- a slack chin strap (2 finger breadth ≈18mm diameter),
- a wearing position that uncovers most of the forehead (Distance eyebrow to leading edge more than two finger breadth ≈ distance from nose tip to helmet rim of 50 mm).

Last, the video analysis indicated that:

- oblique impacts to the forehead or side are very frequent.

The test-setup is shown and explained in Fig. 1. A HIII 5th percentile head with flexible skin was employed, which matches very well with the geometry determined by [30] for 10 year-old (yo) children based on CT pictures. The head was equipped with a chin/throat to accommodate the chin straps (Fig. 2). In order to replicate the influence of the neck and upper body the inertia and the mass of the head were increased as recommended by [31]. Scaling factors of [31] were applied to mass and moment of inertia determined for heads of 10 yo children by [30]. Iyy and mass were increased by 40% and 20%, respectively. Inertia and mass properties can be found in Table VI in the supplementary material (SM). Five helmet models (Fig. 3) were exposed to this test regime in 45 impact tests. Helmet 5 was tested with and without a low friction layer (LFL). Every helmet was tested in frontal and lateral oblique impact, as indicated by the video study. An identical helmet was then tested in the same configuration but in a realistic (misuse) position (Table V in SM). A typical misuse determined in the habitual study was adopted: a slack chin strap (2 finger breadth ≈18mm diameter) and a wearing position that uncovers most of the forehead (Distance eyebrow to leading edge more than two finger breadth ≈ distance from nose tip to helmet rim of 50 mm). Every test was repeated once with a new helmet.

Acceleration was measured at 4 locations (centre of gravity, front, left and top) to determine rotational accelerations indirectly.

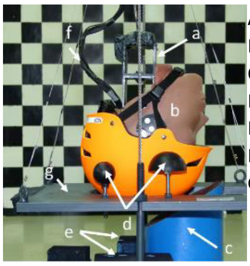

A… Inertiabeam (add-on mass/inertia)
B… Headform HIII 5th with chin/throat
C… Anvil. 30° deg, covered with 80 grain paper
D… Adjustable suspension of helment
E… EPP blocks for decelerating platform
F… Wires for hoisting the platform
G… Platform

Fig. 1: Test setup

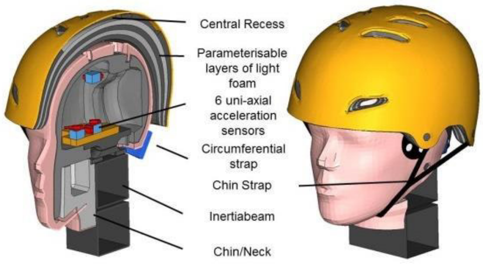

Fig. 2: Helmet fitted to HIII Headform

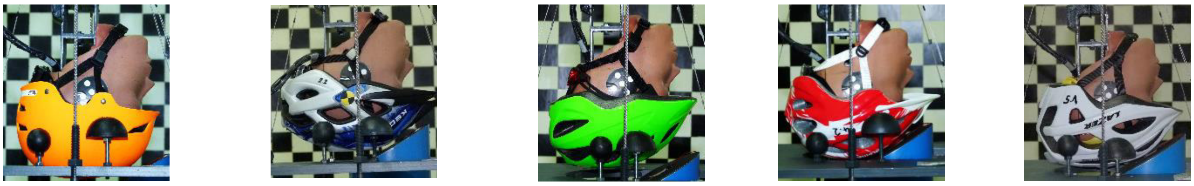

Fig. 3: Tested helmets

Numerical Study

For the numerical study, a hardshell helmet (helmet 1) Kid Size 51 to 55 cm was employed. The baseline helmet is made of expanded polystyrene (EPS) foam with a density of 70 kg/m^3. The EPS liner has a central recess at the top. The outer hard shell is made of Acrylonitrile butadiene styrene (ABS) with a thickness of 2 to 2.2 mm. The EPS foam liner is tied to the ABS hardshell in the parietal area. The remainder is loosely placed into the hardshell. The circumferential strap is 1 mm thick, preferably made of Polyethylene (PE). The chin strap is made of 15mm wide fabric. Consistent with the experiments, the HIII headform was extended by a chin/neck to accommodate the helmet's strap.

The model was created in LS-Dyna code R7.1. The EPS foam liner was modelled using a strain-rate dependent 'Mat_Fu_Chang_Foam', incorporating the findings by [31], [32] and [33]. More details on the modelling are described in the supplementary material. The liner was separated into five consecutive layers. Each layer was assigned a parameter governing the density, the load-function and the tension cut-off stress (a more detailed description of the EPS model and its validation can be found in the SM). The ABS hardshell was modelled using a strain-rate dependent 'Mat_Plasticity' with damage incorporating the findings on strain-rate dependency by [34]. For modelling the chin strap, a 'Mat_Seatbelt' was employed. 1D elements were used, as this simplified the misuse-simulations (no pre-simulation required to provide snug fit of the strap). Two sliprings were rigidly attached to the jawbone. As the model is employed in a parametric study, numerous parameters were introduced in the file-header.

Validation of helmet

The combination of head and helmet was validated against two of the experiments, a frontal and a lateral impact of helmet 1 with ideal fit. The curves match sufficiently well (Fig. 4 and Fig. 5). During validation, the results turned out to be sensitive to the initial position of the head relative to the helmet. Based on pre-test measurements (distance nose tip to helmet leading edge) and pre-test photos, attempts were made to replicate the initial position as closely as possible. It is remarkable that the lateral impact also shows a considerable rotational acceleration about the y-axis, in fact, reaching almost the same peak level as the frontal impact.

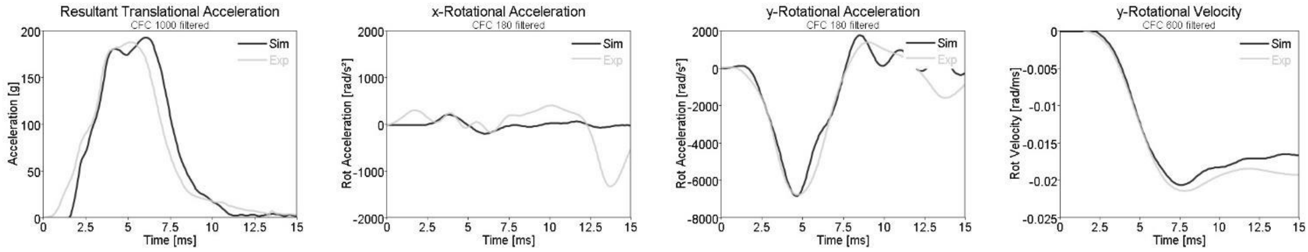

Fig. 4: Validation of Helmet and Head combined. Frontal impact (test 1)

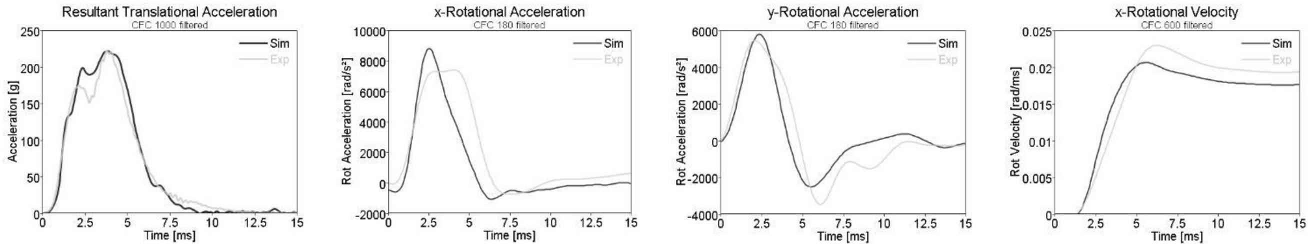

Fig. 5: Validation of Helmet and Head combined. Lateral impact (test 22)

Simulations correlated nicely with the experiment, too, in terms of overall kinematics, helmet deformation and diving motion (Fig. 6 and Fig. 7). In the lateral impact, a little more rebound was observed in the simulation.

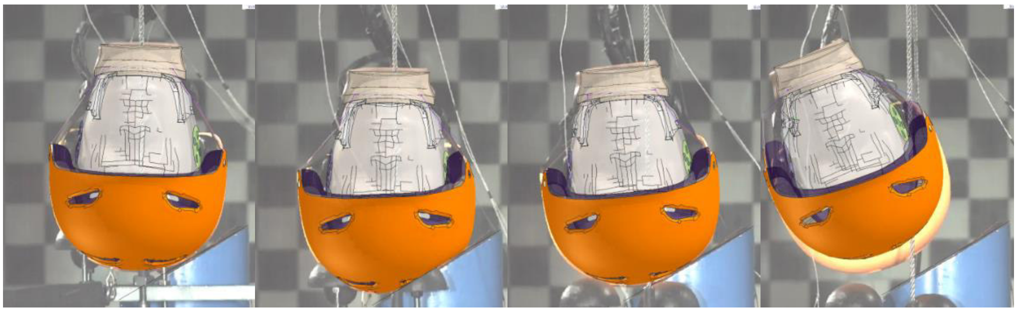
Fig. 6: Simulation versus Experiment - Frame-by-Frame overlay (0, 5, 10 and 25ms). Lateral impact (VS22)

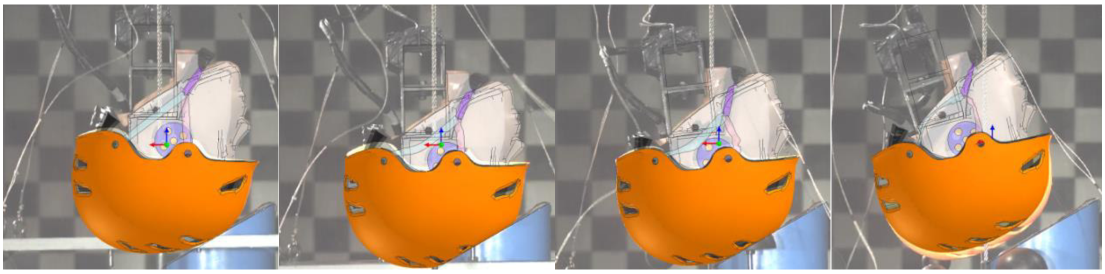
Fig. 7: Simulation versus Experiment - Frame-by-Frame overlay (0, 5, 10 and 25ms). Frontal impact (VS01)

Simulation matrix

The simulation matrix (Fig. 8) consists of 41 impact configurations 'Cfg.' (highlighted in red) and 25 variations 'Var' (highlighted in green), resulting in 1025 runs (A01 through Y41). The impact configurations are a combination of four anvil types (flat, spherical, curbstone, flying – highlighted in orange) and 12 positions of anvil and helmet relative to anvil (highlighted in light blue) A through P. The R-R' plane is taken as a reference for the orientation of the helmet (highlighted by red dotted line in Fig. 9 and Fig. 9). The plane was established by placing the helmet on the head so that it does not interfere with the view planes as defined in EN 1078 and no initial contact penetrations occur (see Fig. 9).

Not every position was tested with all anvils: Pos D, L and P resulted in glancing impacts with the spherical and curbstone anvil. Pos A, I and M were not tested with the flying floor, as they are identical with the flat anvil impacts. Positions U and V are replications of the experimental impact positions, i.e. corresponding to experimental test of helmet 1 frontal and lateral. In the baseline simulations with the non-moving anvils (i.e. curbstone, flat and hemispherical anvil) the head is prescribed an initial velocity in z-direction of -6.5 m/s. In the flying floor simulations, it is assumed that the resultant velocity vector still amounts to 6.5m/s. The velocity is then a function of the equivalent anvil angle. The flying floor impact test is, for example, used by [7].

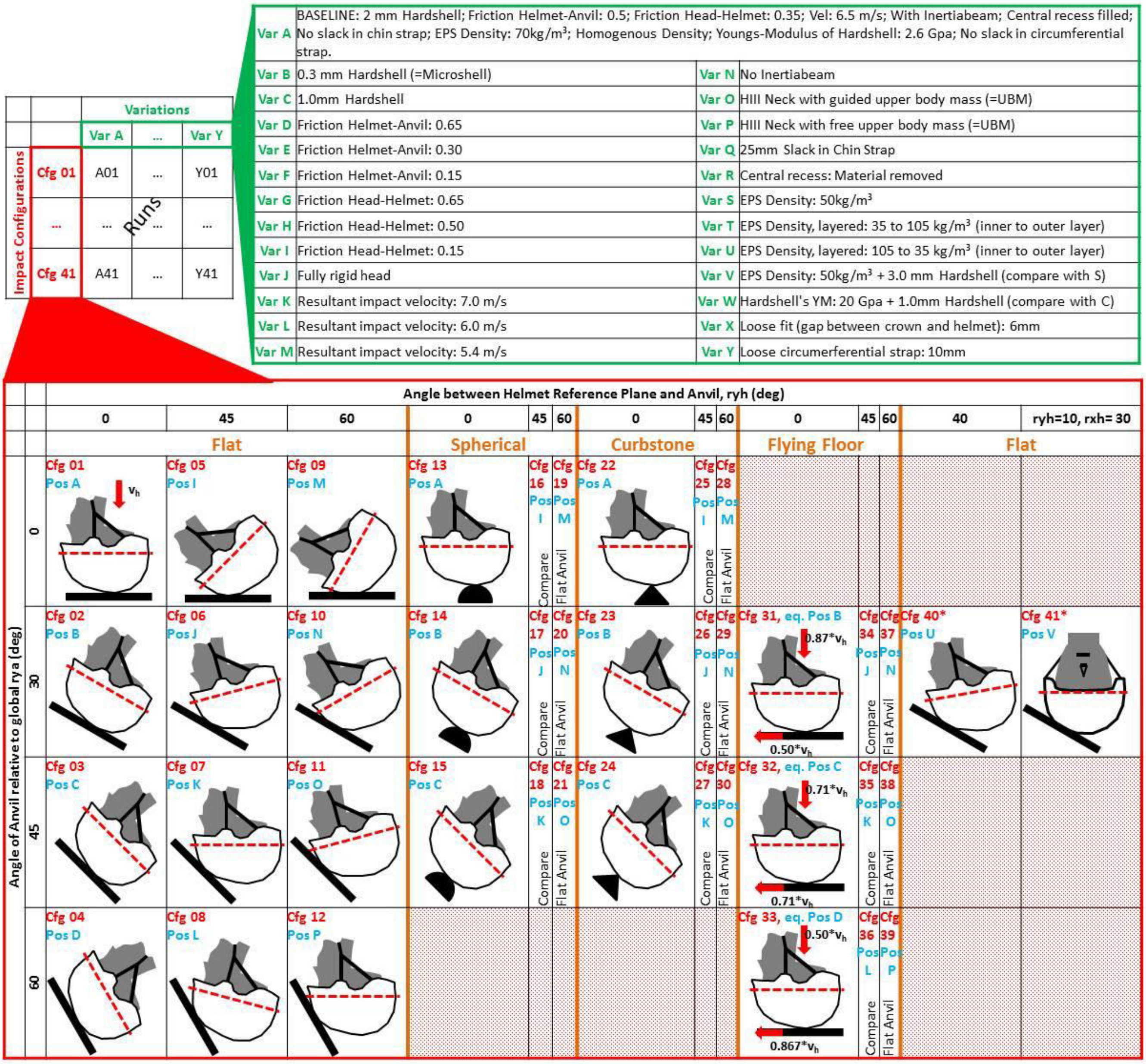

Fig. 8: Simulation matrix: 41 impact configurations (red) versus 25 variations (green)

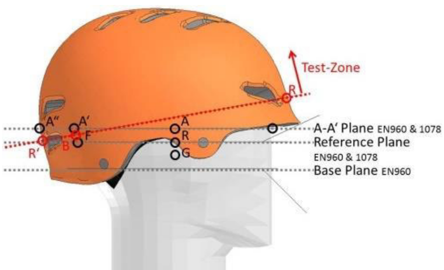

Fig. 9: Planes and Points defined in EN 960 and EN 1078. Test zone lies above R-R' Plane

The variations refer to changes either to the helmet design or the test design (highlighted in green in Fig. 8).

Variation of helmet material: In variant B, a microshell is applied to a hardshell design. Besides that, sectional and material properties of the hardshell and parameters of the EPS liner are varied: A layered EPS is studied in variants T and U. A non-uniform EPS density shall be superior to a homogenous padding [35–37].

Variation of friction: The influence of reducing the coefficient of friction (variants G, H, and I) either between helmet and head or between padding and hardshell were investigated. Helmets equipped with a low-friction layer (LFL) are supposed to mitigate rotational loading [10],[38]. Furthermore the friction between hardshell and anvil was also varied (variants D,E, and F), simulating the effect of peel-off helmet skins [40],[41]

Variation of headform: In variant J, the skin was turned from deformable to rigid, in order to identify the influence of the skin's compliance. In variant N, the inertiabeam used for the experimental tests was removed. In variants 0 and P, an upper body mass (UBM) and a HIII neck was added. The rigid UBM was connected to the lower neck bracket. In variant P, the UBM can move freely. The UBM is assigned the mass and inertia of the HIII 5^{th}'s upper body (m=12.7 kg, Iyy= 129688 kg mm², x= 59 mm, z= -82 mm relative to the central point on the lowermost surface of the neck bracket). In variant O, the UBM was guided, i.e. has only one degree of freedom. The test setup shall replicate the test method used e.g. by Legacy Health Systems (LHS) [10].

Variation of helmet fit: In variant Q, 25 mm belt slack was introduced. Likewise, in variant Y, the circumferential strap was loosened. In variant X, a 6mm gap between helmet and crown of the head was introduced.

Post-Processing of Data

Translational accelerations were filtered with CFC 1000, rotational accelerations with CFC 180 and rotational velocities with CFC 600. Experimental and numerical data were post-processed with the same Altair templex-script. The templex script returns the output parameters shown in the Appendix in Table III and conveys the data to an Excel spreadsheet. The excel spreadsheet calculated the injury risk for several injury criteria listed in Table IV in the Appendix. In total, more than 40 injury risk curves for the 11 head injury criteria and 2 acceleration peak values were found in literature. In this paper, though, only risk curves for AIS 3+ injury of selected criteria were considered, namely a_max, acr_max, HIC36, HIP ,and BrIC based on curves published by [39] and [26], respectively.

Results from experimental testing were prescribed to THUMS v4.0 AF05 pedestrian head and the CSDM was evaluated. CSDM was evaluated for strain limits between 5% ($CSDM_{5\%}$) and 30% ($CSDM_{30\%}$) with a python based postprocessor developed by TU Graz, called 'DynaSaur'.

III. RESULTS

Habitual Study

Among the majority of children (87%), at least one type of misuse was found: The majority of children did not fasten their chin strap properly (60% more than one finger breadth). Furthermore 40% of the children wore their helmets tilted back (more than 2 finger breadth distance to eyebrows), uncovering the forehead.

Experimental Study

Impact testing showed a wide range of protective properties, e.g. the HIC (Fig. 10) ranged from 862 to 1632, BrIC (Fig. 11) from 0.35 (helmet 5 with low friction layer frontal, ideal) to 0.86 (helmet 4 lateral, real).

Helmet position and impact configuration

Marginal differences between real (misuse fit) and ideal fit were found except for helmet 4 and 5. HIC values were higher in the ideal than in the real configuration (Fig. 10). For helmet 1, misuse led to substantially lower BrIC values (Fig. 11). The straps of this helmet are directly attached to the outer hardshell (and are not routed over the circumferential strap as in the microshell helmets). Thus, the head was less constrained and able to rotate more freely relative to the helmet. Generally, higher BrIC values were reached at lateral impacts compared to frontal ones (Fig. 11).

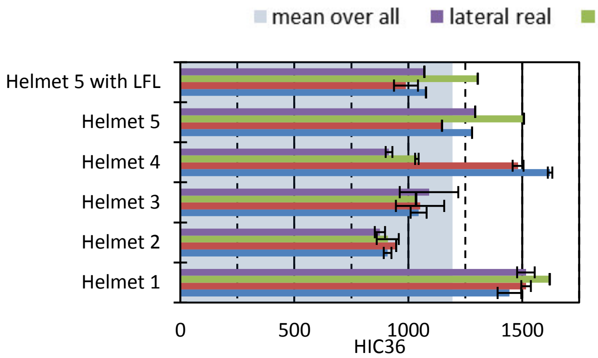

Fig. 10: Overview of HIC values in all tests - whiskers show min. and max. values

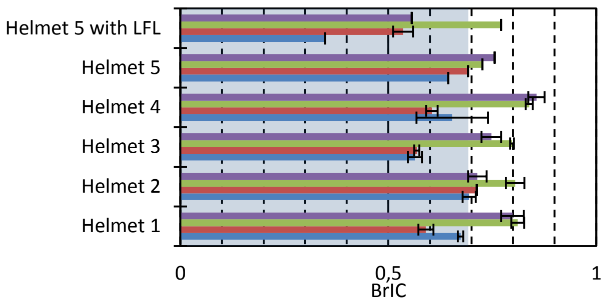

Fig. 11: Overview of BrIC values in all tests - whiskers show min. and max. values

Helmet Design (Low-Friction Layer and Hardshell Helmet)

Helmet 1 (hardshell helmet) and helmet 5 w/ LFL (microshell helmet with low friction layer) were found worst and best performers, exceeding and undercutting the average test results, respectively (Fig. 12). With helmet 5 all injury criteria were significantly lower (p-values determined with student t-test <0.05) compared to helmet 1. Fig. 14 shows what the differences in injury criteria values mean in terms of AIS 3+ injury risk: A reduction of 70% (frontal) and 55% (lateral) based on HIC and 61% (frontal) and 42% (lateral) based on BriC was observed. The $CSDM_{10\%}$ was found 26% in helmet 5 w/ LFL and 0.32% in helmet 1.

Helmet 5 was tested w/ and w/o LFL: The helmet w/ LFL showed significant (p<0.05) lower Injury criteria for mxacrt (p=0.009), HIC36 (p=0.03), HIP (p=0.006), GAMBIT (p=0.01), HIProt (0.042), PRHIC36 (p=0.013), KLC (p=0.028) and PI (p=0.003) (Fig. 13 and Fig. 15). The superior performance of helmet 5 w/ LFL led to a reduction in AIS 3+ injury risk up to 78% and 99 % in $CSDM_{10\%}$. A table with CSDM values is included as supplementary material (Table VII).

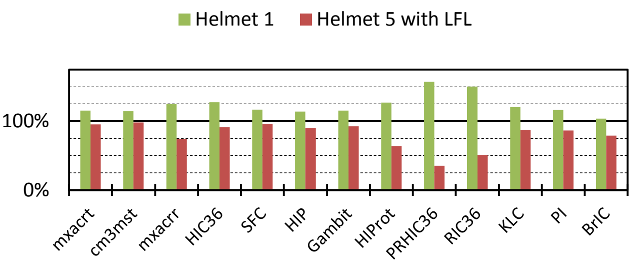

Fig. 12: Difference of mean values of Injury criteria for helmets 1 and 5 with low friction layer - 100% = mean value of all tests

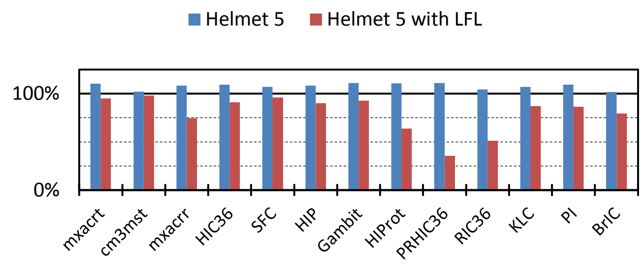

Fig. 13: Difference of mean values of Injury criteria for helmet 5 with and without low friction layer - 100% = mean value of all tests

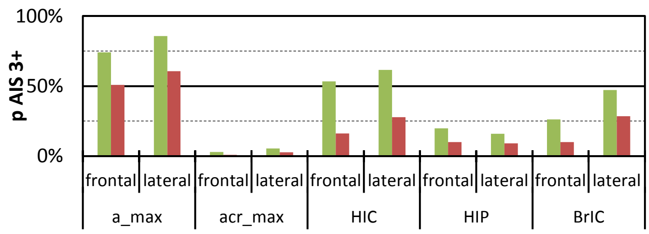

Fig. 14: Risk of AIS 3+ head injuries for Helmet 1 and 5 with low friction layer based on different injury criteria

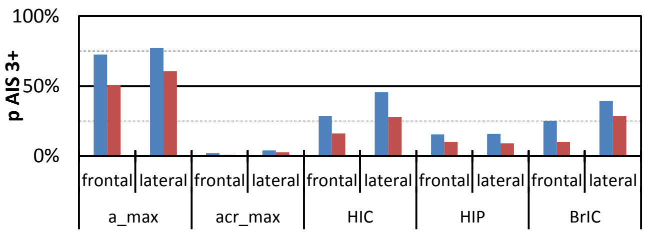

Fig. 15: Risk of AIS 3+ head injuries for Helmet 5 with and without low friction layer based on different injury criteria

Numerical study

The templex script returns numerous parameters. Presenting all outputs would certainly go beyond the scope of this paper. The following relevant output parameters were therefore selected: (1) mxacrt, the maximum resultant translational acceleration, as it is used widely for helmet certification, (2) cn3mst, the continuous 3ms of the translational resultant acceleration; the 3 ms value is used in the Australian helmet certification (3) HIC, as pure translational head injury criterion, (4) BrIC, as one of the most recent representatives of rotational injury criteria, (5) PI and KLC, as recent representatives of combined injury criteria. All data is presented as percentages relative to a baseline simulation (variant A or flat anvil). First, the anvil-types are analysed, then the impact positions and eventually the variations. The flat anvil was selected as reference.

Fig. 16 Selected output parameters by anvil-type (Pos B, C, J, K, N, and O only)

The flying floor basically returned the same results as the flat anvil (Fig. 16), which is no big surprise. It should be mentioned, though, that the flying floor was prescribed a constant velocity. During simulation, external work builds up (roughly 50-75 J). For a physical experiment, this means that the mass of the flying floor should be sufficiently high to provide consistent boundary conditions for all helmets and test-configurations. Tests against the curbstone and the hemispherical impactor returned lower output parameters related to translational and combined loading. For rotational loading criteria (BrIC), the penetrating anvils returned higher values.

Impact-Positions ('Pos') and Anvil Angle

When ranking the positions for each output parameter (see Table I), we find Pos D, U and V among that list four times, followed by I and L three times. D, U, V and L are impacts against an oblique anvil, I is against a horizontal anvil. We can conclude that the experimental impact scenarios U and V (highlighted in bold) were reasonable choices, reflecting two of the worst cases.

TABLE I:
POSITION RANKED 1 TO 3, BY OUTPUT PARAMETER

Rank	mxacrt.	mxacrr.	mxvlrr.	cn3mst.	HIC36.	BrIC	PI.	KLC.
1	**Pos V**	Pos D	Pos L	**Pos U**	**Pos V**	Pos L	Pos D	**Pos V**
2	Pos I	Pos C	Pos D	**Pos V**	Pos I	Pos D	Pos C	**Pos U**
3	**Pos U**	Pos L	Pos P	Pos I	**Pos U**	Pos P	Pos B	Pos M

When analysing the output parameters by anvil angle only (and setting the 30 deg as baseline, i.e. 100%), we can show that peak rotational acceleration and velocity increases with the angle. Consequently, HIC and cn3ms are highest with the 0 deg anvil, while BrIC2 and PI (a combined criteria) is highest in impacts against an oblique anvil (see Fig. 17).

Fig. 17: Selected output parameters versus anvil angle

Next, the results of the 20 variants are summarized. Fig. 18 gives an overview on the changes of the selected output values relative to the baseline simulation A. The variations are grouped in 'Helmet Design', 'Misuse-Fit', 'Headform and Upper body Mass' and discussed in more detail below.

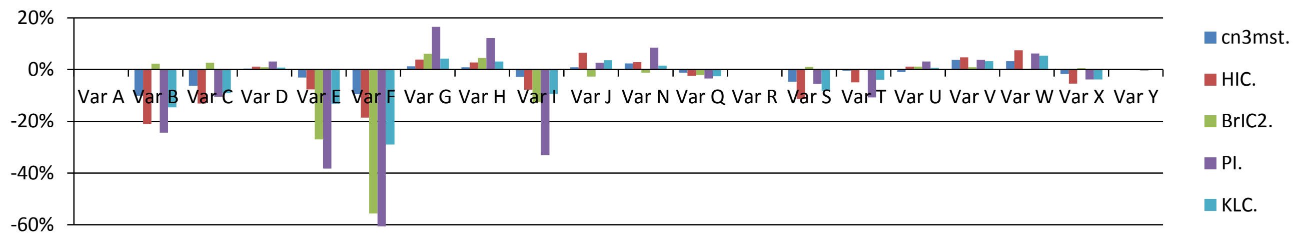

Fig. 18: Selected output parameters by variations (average over all positions, excluding Pos V)

Helmet Design

The 'microshell' (Var B, and C) outperformed the baseline model in almost all criteria (and BrIC2 was only marginally increased). Rotational velocity did not change, but translational accelerations were decreased by approx. 15%, and rotational peak acceleration by 35%. The central recess (Fig. 2) had no effect (Var R). For the helmet under investigation and the selected load cases, a reduction in EPS foam density led to a decrease in output parameters: Peak accelerations (rot and trans) and injury criteria both decreased by 5-10%. A layerwise increasing foam density (Var T) was beneficial, too, mainly for the peak rotational acceleration (-20%). A layerwise decreasing padding density (Var U) led to a minor rise in output parameters. The average densities in variants T and U are 74 and 66 kg/m³, respectively. Hence, total mass differs by +/-8 g relative to the baseline model. We can therefore preclude mass-induced effects.

The sensitivity to the outer hardshell design was further investigated in variants W and X. The findings of variants B and C were re-confirmed: A thicker or stronger hardshell is adverse to almost all parameters, except for BrIC and peak rotational velocity – at least for the investigated impact boundary conditions.

In Var D through H the effect of friction was investigated: Helmet design measures might increase the coefficient of friction between head and helmet and lead to a considerable increase in parameters, mainly related to peak rotational acceleration (+20% in Var G). Vice versa, the loads were reduced. Comparing variations in helmet-anvil (D, E, F) and head-helmet (F, G, H) friction, it appears that the latter has less effect in terms of rotational peak velocity. Therefore, KLC, BrIC2, PI and HIP appear less sensitive to changes in the head-helmet, compared to helmet-anvil friction. Additional simulations were performed to cover an entire field of these two coefficients of friction, which are shown in the supplementary material (Fig. 23). The HIC surface is (in terms of shape) very similar to the maximum translational acceleration. The BrIC2, on the other hand, shows the same surface shape as the maximum rotational velocity. It is no big surprise, then, that best results were achieved when both frictional coefficients were reduced. Interestingly, the cn3ms (not shown) does not show robust reductions (rather a flat surface, with a max. reduction of 7%).

Misuse fit

A loose fit, i.e. a gap between the head's crown and the helmet, was simulated in variant X. Surprisingly this 'misuse' case provided better results than the baseline. Higher frictional energies were observed in these simulations. Adding slack to the chin strap (Var Q) led to a 5% decrease in rotational peak acceleration. All injury criteria decreased marginally (2.5 to 3.5%). A loose circumferential strap was found to have no effect on the simulation's outcome (Var Y).

Headform and upper body mass

Using a fully rigid headform (Var J) had a comparatively small effect. Rotational accelerations were decreased by 7%. Peak translational accelerations remained virtually unchanged (+1.5%). HIC, KLC and PI increased by 4-6%. In the numerical study, the influence of the inertiabeam shall be compared to tests where the head was attached to either a free moving or a guided upper body mass through a HIII neck. Removing the inertiabeam (Var N) led to an 11% increase in rotational accelerations. Rotational velocity-change remained virtually unchanged. Among injury criteria, it mainly affected the PI, which was increased by 8%.

Evaluation of the peak values showed that rotational loading is much higher with an upper body mass (UBM). Fig. 19 compares the four variants: without inertiabeam (Var N), with inertiabeam (Var A), with HIII neck and free UBM (Var P), and with guided UBM (Var O) for one position (Pos U – see Fig. 8). For the kinematics of these variants, please refer to Fig. 24 of SM.

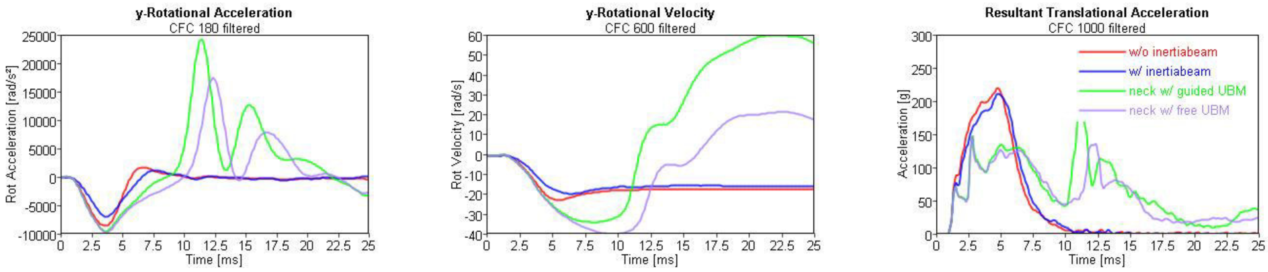

Fig. 19: Effect of neck, upper body mass and inertiabeam (Pos U)

For the impact against the 30 deg anvil (Pos U), the inertiabeam does not seem to provide more realistic rotational loading. For some of the positions (e.g. Pos A and B – please refer to the SM, i.e. Fig. 25 and Fig. 26), though, the inertiabeam is beneficial to the replication of rotational accelerations in the very first phase of impact, i.e. in the first 5 ms. Going back to the impact against the 30 deg anvil (Pos U): the head-only (Var N) and upper body mass tests (Var O, P) correlate sufficiently well in the first 5 ms (see Fig. 19). In the test with the upper body mass, though, rotational velocity builds up for another 5 ms, reaching a peak value almost twice as high. The translational accelerations are considerably smaller in the tests with the UBM. When comparing the kinematics of the four variants (Fig. 24 in SM) more crush (which indicates more traction and thus a higher rotational peak velocity), longer contact duration and smaller post-impact head velocity were observed when the UBM was present. With the guided UBM (see 3rd row from left in Fig. 24), the neck snaps through after 15 ms (from flexion to extension).

Fig. 20 shows the contact forces, with and without UBM. Contact force in the 30 deg impact (Pos U) is 48% higher with UBM. When considering all impact constellations under investigation (Pos A-L), the contact forces increased in the range from 40 to 67%. For other impact positions (Pos A-D,I-L), the curves can be found in the SM (see Fig. 25 and Fig. 26). Since an increased contact force can be achieved by adding mass to the impactor, another 10 simulations were run, randomly adding a point mass close to the headform COG. The best correlation (among these 10) with the free UBM was achieved by adding 7 kg 37 mm above the COG (Fig. 21): The rotational velocity was increased and the maximum translational acceleration decreased, showing a better correlation with the free UBM simulations. (Remark: An optimisation study on add-on mass and its location relative to the COG was not performed. This will be carried out in a future study, using a child human model for comparison).

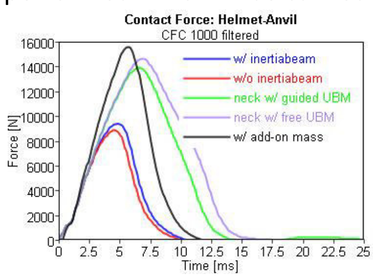

Fig. 20: Effect of neck, upper body mass and inertiabeam (Pos U) on contact force

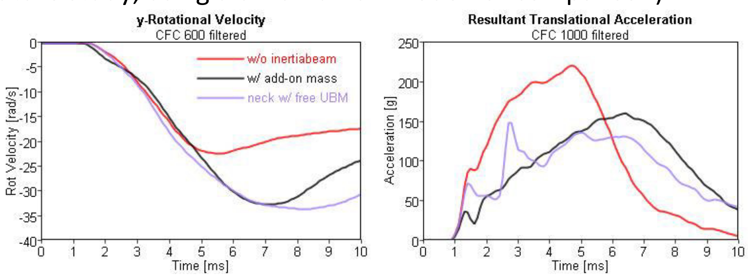

Fig. 21: Effect of 7 kg add-on mass on rotational velocity and translational acceleration

Though a better correlation in terms of peak contact force (Fig. 20), rotational velocity and translational acceleration (Fig. 21) can be achieved by increasing the headform's mass, the contact duration (Fig. 20) is still underestimated and the post-impact velocity overestimated, because a reasonable amount of the impact energy is converted into internal energy stored in the neck. In the free UBM simulations, 50% of the delta in kinetic energy (260 J) is stored in the neck (133 J), while only 30% goes into the deformation of the foam liner (80 J).

IV. DISCUSSION

Experimental Test-Setup

In the experiments it was surprisingly difficult to exactly reproduce the impact location for some helmets (helmet 2 and 4), which led to rather mediocre repeatability (Fig. 10 and Fig. 11). In free-fall, the wiring led to small movements of the helmet prior to impact. A wireless data-acquisition is highly recommendable for reproducible testing. Experimental tests have shown that measuring head rotational acceleration using translational acceleration sensors in tests with relatively hard contact is not straightforward. Recent injury criteria (BrIC, KLC) are a function of rotational velocity change. Hence, the use of gyro sensors is highly recommendable.

Recommendations for a future testing protocol are summarised in Table II.

TABLE II:
DISCUSSION OF TEST PARAMETERS FOR HELMET IMPACT TESTING

	EN 1078	applied test protocol (based on)	Recommendations based on this study
impact velocity	5.4 m/s	6.5 m/s ([12],[13])	
anvil	flat anvil or kerbstone smooth surface	30° anvil covered with abrasive paper (μ=0.5) [28]	30° was found to be a good trade off between rotational and translational loading
Setup	Free fall impactor	Free fall impactor [28]	Free fall impactor. Flying floor too complex given the benefit
headform	rigid EN 960 headform smooth surface	modified HIII 5th head [11],[29], compliable and sticky skin	Headform shall provide realistic friction between helmet and headform
headform mass	4.1 kg (size: 535)	4.3 kg (3.6 kg +20%)[30],[41]	Add-on mass to account for UBM has to be reinvestigated using child human model
impact position	selected by test inspector	RR' plane 10 degree aligned - frontal and lateral impact	Combination of pre-defined impact points: (1) frontal and lateral oblique impact and (2) test inspector selected impact against horizontal anvil
helmet fit / misuse	ideal	ideal and realistic (misuse)	Ideal sufficient
threshold	Max. resultant acceleration <250 g	11 injury criteria were evaluated	Evaluation of AIS 3+ risk based on BrIC and HIC as a first step – sophisticated combined criterion for preadolescents needed

Headform and attached body mass

Based on the variation-analysis we hypothesize that it is necessary to increase mass, without interfering with the inertia too much, to replicate the tests with the upper-body mass more closely (at least for the first 10-15 ms). Add-on mass and its position will have to be selected depending on the impact angle (i.e. angle between velocity vector and anvil) or as a function of an effective lever arm length.

Compared to simulations with HIII neck and UBM, it turned out that add-on mass used in the experimental study were too low, though. However, the Hybrid III neck is not validated for impact configurations used in this study. To determine an effective impactor mass, simulations should be carried out with an advanced human body FE model. This will be done as soon as CHARM-10 (a model of a 10yo) is available.

The selected scaling factors by [30] were based on observations in terms of rotational acceleration and not on rotational velocity. Recent head-injury criteria (KLC, BrIC) are based on rotational velocity change, though. Therefore in future helmet testing focus shall be put on the correct replication of the velocity change.

Misuse

Numerical and experimental studies showed that a slack chin strap led to generally lower output parameters. However, the impact tests did not consider the pre-impact phase, during which the chin strap ensures that the helmet remains on the head. The chin strap should be tightened sufficiently to hold the helmet in place in the pre-impact phase and the helmet should cover as much of the neurocranium as possible. It is important to protect the forehead: Several studies [3],[13],[40] and our video analysis showed that the forehead is a common impact point. Cyclists wearing their helmet tilted back (observed among 40% of the children) are likely to be unprotected in case of a frontal impact.

Helmet Design

Surprisingly, the layer-wise increasing padding density was only marginally effective in reducing peak translational accelerations, though, this approach was found to be effective in other publications [35–37] The manufactures realise a density increasing with thickness is realized through two 'dented' layers of foam which probably influence the benefit. It can be presumed, though, that a layered padding provides protection over a wider impact velocity-range because yielding is already initiated at lower velocities. Thus, energy is absorbed where single-layer helmets remain undeformed

Injury Criteria

In this study, a total of 11 head injury criteria and 40 underlying injury risk curves were considered. Based on the current status of the project, it is not possible to recommend a specific set of injury criteria for experimental helmet testing, mainly because experimental testing fails in replicating the effect of the upper body.

Evaluating only peak linear accelerations means neglecting the range of advanced injury criteria available today. To bring helmet testing to a new level requires a holistic evaluation including the need for analysis of rotational velocities. Further research is needed to define appropriate thresholds for preadolescents.

V. CONCLUSIONS

- Most children wear their helmets tilted too far towards the neck, exposing the forehead, which is a frequent impact location.
- Other misuse, i.e. a slack chin strap or a slack circumferential strap, was found to have no adverse effect on impact attenuation performance. Nonetheless, the straps should be sufficiently tightened to hold the helmet in place in the pre-impact phase.
- Tests as performed currently according to EN 1078 overestimate translational accelerations.
- If the same impactor (EN 960) were used in oblique impact, rotational velocity change would be underestimated.
- A new helmet testing protocol was applied: A helmet was fitted to a headform with flexible skin and add-on mass/inertia to account for upper body mass. Frontal and lateral impacts against oblique anvil considering misuse were conducted. Generally, plausible results were observed. Clear 'winners' and 'losers' were observed.
- The approach of adjusting the mass/inertia in order to replicate the influence of the UBM is feasible. At least this would provide a better correlation within the first 10-15 ms of the impact.
- Output parameters were found to be sensitive to the coefficient of friction between head and helmet and helmet and anvil. Therefore, the headform's skin is crucial in replicating human skin in terms of frictional interface properties and a realistic friction of the anvil is needed.
- A 30° degree anvil angle together with a 10° deg R-R' plane was found to be a good trade-off between rotational and translational loading.
- As long as the test is not biofidelic in terms of rotational and translational loading, there is no point in using advanced head injury criteria (e.g. KLC, BrIC, PI).

VI. ACKNOWLEDGEMENT

The authors would like to thank the Austrian Ministry for Transport, Innovation and Technology for funding the study. Further, we would like to acknowledge the use of HPC resources provided by the ZID at Graz University of Technology, Austria. The authors are grateful to Lena Klug and Marlene Wallisch for their help with the habitual study.

VII. REFERENCES

[1] Statistik Austria. Traffic Accident Statistics 2007-2011.

[2] Statistik Austria. Demographic Statistics 2007-2011.

[3] Depreitere, B., Van Lierde, C., Maene, S., Plets, C., Vander Sloten, J., Van Audekercke, R. et al. Bicycle-related head injury: a study of 86 cases. *Accident Analysis & Prevention*, 2004, 36(4):561–7.

[4] Hagel, B.E., Lee, R.S., Karkhaneh, M., Voaklander, D. and Rowe, B.H. Factors associated with incorrect bicycle helmet use. *Injury Prevention*, 2010, 16(3):178–84.

[5] Romanow, N.R., Hagel, B.E., Williamson, J. and Rowe, B.H. Cyclist head and facial injury risk in relation to helmet fit: A case-control study. *Chronic Diseases and Injuries in Canada*, 2014, 34(1):1–7.

[6] Mihora, D., Hutchinson, J., Friedman, K., Valente, J., Flanagan, T., Jr, A.S. et al. Bicycle helmet retention system testing and evaluation. *International Journal of Crashworthiness*, 2007, 12(3):211–5.

[7] Aare, M. and Halldin, P. A New Laboratory Rig for Evaluating Helmets Subject to Oblique Impacts. *Traffic Injury Prevention*, 2003, 4(3):240–8.

[8] McIntosh, A.S., Lai, A. and Schilter, E. Bicycle Helmets: Head Impact Dynamics in Helmeted and Unhelmeted Oblique Impact Tests. *Traffic Injury Prevention*, 2013, 14(5):501–8.

[9] Mills, N.J. and Gilchrist, A. Oblique impact testing of bicycle helmets. *International Journal of Impact Engineering*, 2008, 35(9):1075–86.

[10] Hansen, K., Dau, N., Feist, F., Deck, C., Willinger, R., Madey, S.M. et al. Angular Impact Mitigation system for bicycle helmets to reduce head acceleration and risk of traumatic brain injury. *Accident Analysis & Prevention*, 2013, 59:109–17.

[11] Willinger, R., Deck, C., Halldin, P. and Otte, D. Towards advanced bicycle helmet test methods. *Proceedings, International Cycling Safety Conference 2014*, 2014, Gothenburg, Sweden.

[12] Bourdet, N., Deck, C., Serre, T., Perrin, C., Llari, M. and Willinger, R. In-depth real-world bicycle accident reconstructions. *International Journal of Crashworthiness*, 2014, 19(3):222–32.
[13] Bourdet, N., Deck, C., Carreira, R.P. and Willinger, R. Head impact conditions in the case of cyclist falls. *Proceedings of the Institution of Mechanical Engineers, Part P: Journal of Sports Engineering and Technology*, 2012, 226(3-4):282–9.
[14] Versace, J. A Review of the Severity Index. 1971 Feb, SAE International, Warrendale, PA. 771–96 Report No.: 710881.
[15] Deck, C., Baumgartner, D. and Willinger, R. Influence of rotational acceleration on intracranial mechanical parameters under accidental circumstances. *Proceedings of IRCOBI Conference*, 2007, Maastricht, Holland.
[16] Feist, F., Gugler, J., Arregui-Dalmases, C., del Pozo de Dios, E., López-Valdés, F., Deck, C. et al. Pedestrian Collisions with Flat-Fronted Vehicles: Injury Patterns and Importance of Rotational Accelerations as a Predictor for Traumatic Brain Injury (TBI). *Proceedings of the 21st ESV Conference*, 2009, Stuttgart, Germany.
[17] Arregui-Dalmases, C., Lopez-Valdes, F.J. and Segui-Gomez, M. Pedestrian injuries in eight European countries: an analysis of hospital discharge data. *Accident Analysis & Prevention*, 2010, 42(4):1164–71.
[18] King, A.I., King H. Yang, Zhang, L. and Hardy, W. Is head injury caused by linear or angular acceleration? *Proceedings of IRCOBI Conference*, 2003, Lisbon.
[19] Kleiven, S. Predictors for traumatic brain injuries evaluated through accident reconstructions. *Stapp Car Crash Journal*, 2007, 51:81–114.
[20] Newman, J.A. A generalized acceleration model for brain injury threshold (GAMBIT). *Proceedings of IRCOBI Conference*, 1986, Zürich.
[21] Newman, J.A., Shewchenko, N. and Welbourne, E. A proposed new biomechanical head injury assessment function - the maximum power index. *Stapp Car Crash Journal*, 2000, 44:215–47.
[22] Marjoux, D., Baumgartner, D., Deck, C. and Willinger, R. Head injury prediction capability of the HIC, HIP, SIMon and ULP criteria. *Accident Analysis & Prevention*, 2008, 40(3):1135–48.
[23] Kleiven, S. Influence of Impact Direction on the Human Head in Prediction of Subdural Hematoma. *Journal of Neurotrauma*, 2003, 20(4):365–79.
[24] Kimpara, H. and Iwamoto, M. Mild traumatic brain injury predictors based on angular accelerations during impacts. *Annals of Biomedical Engineering*, 2012, 40(1):114–26.
[25] Takhounts, E.G., Hasija, V. and Ridella, S.A. Kinematic Rotational Brain Injury Criterion (BRIC). 2011, National Highway Traffic Safety Administration. Report No.: 11-0263.
[26] Takhounts, E.G., Craig, M.J., Moorhouse, K., McFadden, J. and Hasija, V. Development of brain injury criteria (BrIC). *Stapp Car Crash Journal*, 2013, 57:243–66.
[27] Takhounts, E.G., Eppinger, R.H., Campbell, J.Q., Tannous, R.E., Power, E.D. and Shook, L.S. On the Development of the SIMon Finite Element Head Model. *Stapp Car Crash Journal*, 2003, 47:107–33.
[28] Milne, G., Deck, C., Bourdet, N., Allinne, Q., Gallego, A., Carreira, R.P. et al. Assessment of Bicyclist Head Injury Risk under Tangential Impact Conditions. *Proceedings of IRCOBI Conference*, 2013, Gothenburg, Sweden.
[29] Gilchrist, A. and Mills, N.J. Protection of the side of the head. *Accident Analysis & Prevention*, 1996, 28(4):525–35.
[30] Ghajari, M., Peldschus, S., Galvanetto, U. and Iannucci, L. Effects of the presence of the body in helmet oblique impacts. *Accident Analysis & Prevention*, 2013, 50:263–71.
[31] Uftring, J. and Scholpp, G. Validierung von dehnratenabhängigem Schaummaterial für verschiedene Temperaturen. 2005, dynamore, Bamberg.
[32] Schraad, M.W. and Harlow, F.H. A stochastic constitutive model for disordered cellular materials: Finite-strain uni-axial compression. *International Journal of Solids and Structures*, 2006, 43(11–12):3542–68.
[33] Cui, L., Kiernan, S. and Gilchrist, M.D. Designing the energy absorption capacity of functionally graded foam materials. *Materials Science and Engineering: A*, 2009, 507(1–2):215–25.
[34] Louche, H., Piette-Coudol, F., Arrieux, R. and Issartel, J. An experimental and modeling study of the thermomechanical behavior of an ABS polymer structural component during an impact test. *International Journal of Impact Engineering*, 2009, 36(6):847–61.
[35] Kiernan, S., Cui, L. and Gilchrist, M.D. Propagation of a stress wave through a virtual functionally graded foam. *International Journal of Non-Linear Mechanics*, 2009, 44(5):456–68.
[36] Fernandes, F.A.O. and Alves de Sousa, R.J. Motorcycle helmets—A state of the art review. *Accident Analysis & Prevention*, 2013, 56:1–21.

[37] Morgan, D.E. and Szabo, L.S. Improved Shock Absorbing Liner for Helmet. 2001, Australian Transport Safety Bureau.

[38] MIPS AB. "Brain Protection System". Internet: [http://mipshelmet.com/] 2015 [05/22/2015]

[39] Peng, Y., Yang, J., Deck, C., Otte, D. and Willinger, R. Development of head injury risk functions based on real-world accident reconstruction. *International Journal of Crashworthiness*, 2013, 19(2):1–10.

[40] Ching, R.P., Thompson, D.C., Thompson, R.S., Thomas, D.J., Chilcott, W.C. and Rivara, F.P. Damage to bicycle helmets involved with crashes. *Accident Analysis & Prevention*, 1997, 29(5):555–62.

[41] Loyd, A.M., Nightingale, R., Bass, C.R., Mertz, H.J., Frush, D., Daniel, C. et al. Pediatric head contours and inertial properties for ATD design. *Stapp Car Crash Journal*, 2010, 54:167–96.

[42] Gadd, C.W. Use of a Weighted-Impulse Criterion for Estimating Injury Hazard. 1966 Feb, SAE International, Warrendale, PA. Report No.: 660793.

[43] Vorst, M.V., Stuhmiller, J., Ho, K., Yoganandan, N. and Pintar, F. Statistically and Biomechanically Based Criterion for Impact-Induced Skull Fracture. *Annual Proceedings / Association for the Advancement of Automotive Medicine*, 2003, 47:363–81.

VIII. APPENDIX

TABLE III

OUTPUT-PARAMETERS EVALUATED BY TEMPLEX SCRIPT.

Output-Parameters	**Description**
mxacxt, mxacyt, mxaczt, mxacrt	Peak translational accelerations (x,y,z, Resultant)
mxacxr, mxacyr, mxaczr, mxacrr	Peak rotational accelerations (x,y,z, Resultant)
mxvlxr, mxvlyr, mxvlrr	Peak rotational velocity (x,y, Resultant)
cm3mst, cm6mst, cn3mst	Cumulative 3ms, 6ms and contiguous 3ms translational acceleration
cm3msr, cn3msr	Cumulative 3ms and contiguous 3ms rotational acceleration
HIC36, GSI, SFC	Head Injury Criteria – translational loading only
PRHC36, RIC36, BrIC (new)	Head Injury Criteria – rotational loading only
HIP, PI, Gambit, wPCS, KLC, BRIC (old)	Head Injury Criteria – combined loading
BltFoR, NckFoZ, NckFoR, NckMoY, NckMoX	Simulation only: Resultant belt force, forces and moments in upper neck load cell
mxCNTE,mxINTE, mxEXTE, mxTOTE, …	Simulation only: Energies (Friction, Internal, External, Total)

TABLE IV:

INJURY CRITERIA

Criteria	Equation	Constants	Injury level / type
GSI [42]	$GSI = \int_0^T a(t)^{2.5} dt$		
HIC [14]	$HIC = (t_2 - t_1) \cdot max\left[\frac{1}{(t_2 - t_1)}\int_{t_1}^{t_2} a(t)dt\right]^{2.5}$		Skull fracture, concussion
GAMBIT [20]	$GAMBIT = \left[\left(\frac{a(t)}{a_c}\right)^n + \left(\frac{\alpha(t)^m}{\alpha_c}\right)\right]^{\frac{1}{k}}$	$a_c = 250g$ $\alpha_{cr} = 25\ krad/s^2$ $k = m = n = 2$	1=50% risk of AIS 3+
HIP [21]	$Power = P = \sum m a_i \int a_i\, dt + \sum I_{ii} \cdot \alpha \cdot \int \alpha_i\, dt$	m=4.3kg I_{xx}=14500 kgmm² I_{yy} = 23000 kgmm² I_{zz} = 15700 kgmm²	Concussion
PI [23]	$PI = \sum C_i m a_i \int a_i\, dt + \sum C_i I_{ii} \cdot \alpha \cdot \int \alpha_i\, dt$	$C_{x+} = 1.25$, $C_{x-} = 0.62$ $C_y = 1$ $C_{z+} = 0.69$, $C_{z-} = 0.00$ $C_{x\_rot} = 1.25$, $C_{y\_rot+} = 1.56$, $C_{y\_rot-} = 4.69$ $C_{z\_rot} = 1.37$	Subdural haematomas
BRIC [25]	$BRIC = \frac{\omega_{max}}{\omega_{cr}} + \frac{\alpha_{max}}{\alpha_{cr}}$	$\omega_{cr} = 46.41\ rad/s$ $\alpha_{cr} = 39.774\ krad/s^2$	DAI AIS 1- AIS 5
BrIC [26]	$BrIC = \left(\frac{\omega_{\max\_x}}{\omega_{cr\_x}}\right)^2 + \left(\frac{\omega_{\max\_y}}{\omega_{cr\_y}}\right)^2 + \left(\frac{\omega_{\max\_z}}{\omega_{cr\_z}}\right)^2$	$\omega_{cr_x} = 66{,}25$ $\omega_{cr\_y} = 56{,}45$ $\omega_{cr\_z} = 42{,}87$	Brain Injury AIS 1- AIS 5
PRHIC [24]	$PRHIC = (t_2 - t_1) \cdot max\left[\frac{1}{(t_2 - t_1)}\int_{t_1}^{t_2} HIP_{rot} dt\right]^{2.5}$	$HIP_{rot} = \sum I_{ii} \cdot \alpha \cdot \int \alpha_i\, dt$	Mild TBI
RIC [24]	$RIC = (t_2 - t_1) \cdot max\left[\frac{1}{(t_2 - t_1)}\int_{t_1}^{t_2} \alpha(t)dt\right]^{2.5}$		Mild TBI
KLC [19]	$KLC = 0.004718 \cdot \omega_r + 0.000224 \cdot HIC_{36}$		concussion
SFC [43]	$SFC = \frac{\int_{t_1}^{t_2} a(t)dt}{(t_2 - t_1)}$	$(t_2 - t_1)\max 15\ ms$	Skull fracture

Testing of bicycle helmets for preadolescents
Supplementary Material

A. *Experimental Testing*

TABLE V:
TESTED HELMET FITS

Ideal Fit (EN 960 and helmet manual)	Real (Misuse) Fit
	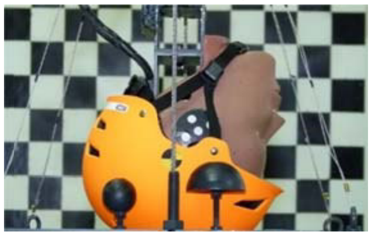
Chin straps as tight as possible	Loose chin strap (2 finger breadth between strap and chin – a round gauge with 18 mm diameter was used as spacer)
Tight "V-Straps" straps under ears	Loose "V-Straps"
Helmet covers forehead (1 finger's breadth distance to eyebrows – 20 mm from tip of the nose to rim of helmet)	Helmet tilted backwards (3 finger's breadth distance to eyebrows - 50 mm from tip of the nose to rim of helmet)
Adjustment screw fastened	Loose Adjustment screw (1 turn loosened)

TABLE VI
INERTIA AND MASS PROPERTIES

	mass [kg]	I_{xx} [kg*m²]	I_{yy} [kg*m²]	I_{zz} [kg*m²]
HIII 5% female	3,67	1.22E-02	1.62E-02	1.30E-02
EN 960	4,1			
10 yo child according to Loyd et al.,	3,62	1,35E-2	1,64E-2	1,19E-2
Percentage increase proposed by [30]	20%		40%	
Adapted Properties used for frontal impacts in experimental tests	4,3	9,32E-3	2,3E-2	1,57E-2

B. *EPS-Modelling*

The load functions are a function of the density, based on the constitutive model described by [32]. The uniaxial compression characteristics of disordered cellular materials can be separated into three phases: In phase 1, the buckling behaviour of cell-walls dominate. When the yield strain ε_1 is reached, the material softens, and the tangential modulus reaches a minimum. In phase 2, an increasing number of cell-wall contacts let the tangential modulus increase with strain until compaction strain ε_2 is reached. In phase 3, the cellular foam is fully compacted and the parent material governs the behaviour. For $\varepsilon \le 0$, the tangential modulus can be described through a function (Eq. 1), where H is the Heaviside function, and A0 and A1 are the form-parameters derived by [33] under the assumption of a Poisson's ratio of 0 (Eq. 3 and Eq. 4), where subscript 0 refers to the expanded (foamy) material, while subscript S refers to the unexpanded parent material. E0, E1 and σ1 as a function of density (Eq. 5, Eq. 6 and Eq. 7) were derived through regression of compression tests performed with material samples with a density between 18 and 320 kg/m³. (Remark: unit-system is mm, kg, ms). Compaction strain ε_2 as function of parent and expanded material is based on a recommendation by [32]– see Eq. 9.

$$E^c(\epsilon) = \frac{[A_0 H(\epsilon - \epsilon_1) + A_1 H(\epsilon_1 - \epsilon) + (1 - A_1) H(\epsilon_2 - \epsilon)] E^s {\phi_0}^2}{(1+\epsilon)^2} \quad \text{Eq. 1}$$

$$\phi_0 = \frac{\rho_s}{\rho_0} \quad \text{Eq. 2}$$

$$A_0 = \frac{E_0 {\rho_s}^2}{E_S {\rho_0}^2} \quad \text{Eq. 3}$$

$$A_1 = \frac{E_1 {\rho_s}^2}{E_S {\rho_0}^2}(1+\varepsilon_1)^2 \quad \text{Eq. 4}$$

$$E_0(\rho_0) = 234262\ \rho_0 \quad \text{Eq. 5}$$

$$E_1(\rho_0) = \frac{23346\ \rho_0 - 3\ 10^{-5}}{4.5} \quad \text{Eq. 6}$$

$$\sigma_1(\rho_0) = 6850.1\ \rho_0 + 1\ 10^{-5} \quad \text{Eq. 7}$$

$$\varepsilon_1 = \frac{\sigma_1(\rho_0)}{E_0(\rho_0)} \quad \text{Eq. 8}$$

$$\varepsilon_2(\rho_0) = 1 - \frac{\rho_s}{\rho_0} \quad \text{Eq. 9}$$

Finally, the parameterisable load functions were compared to quasi-static experimental test data and the functions were found to correlate very well. For modelling, the EPS foam Mat_Fu_Chang_Foam (Mat_083) was employed [31]. Based on the findings by Croop and Lobo [46], it was assumed that rate behaviour is linear with the logarithm of strain rate. A 40% increase over 4 decades of strain rates (up to 0.1 ms^{-1}) as well as the same shape and hysteretic factors (5 and 1%, respectively) were assumed for all foam densities.

Alternatively, Mat_057 (low density foam) was employed. Modelling the strain rate effects using a one-term Prony series is not straightforward. In the validation experiments, the material was either too compliant at low strains or overly stiff at higher strains, or the increase over the logarithmic strain rate was not linear. Using a least-square method, the best correlation was achieved with the following parameters: E_D=3.5e-4 GPa, β_1=3.5e-3 ms^{-1}. Based on the results of the validation experiments, Mat_083 was favoured over Mat_057.

The EPS material model was validated in a simple experiment: A hemispherical free fall impactor (r=54mm, m=3.225kg) impacts a 20mm thick stripe of EPS (40mm wide, 150mm long) at 2.78 m/s. Fig. 22 shows the comparison between experiment and simulation. Apparently, Mat_83 provides a very nice correlation.

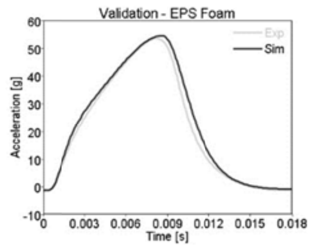

Fig. 22: Validation of EPS material

C. Results of experimental testing

TABLE VII
CSDM ANALYSIS

Helmet	Type	Config.	CSDM Strain limit 0.05	0.1	0.15	0.2	0.25
Helmet 1	Frontal	ideal	85.41	25.64	2.05	0.23	0.06
Helmet 1	Frontal	real	80.55	14.49	0.80	0.15	0.00
Helmet 5 with LFL	Frontal	ideal	30.68	0.32	0.00	0.00	0.00
Helmet 5 with LFL	Frontal	real	66.55	3.00	0.15	0.00	0.00
Helmet 5	Frontal	ideal	84.91	27.68	2.18	0.22	0.04
Helmet 1	Lateral	ideal	84.26	26.02	1.81	0.19	0.03
Helmet 1	Lateral	real	86.78	20.81	3.61	0.41	0.03
Helmet 5 with LFL	Lateral	ideal	80.72	15.62	2.66	0.26	0.02
Helmet 5 with LFL	Lateral	real	89.34	25.92	4.20	0.47	0.06

D. Results of numerical study on friction properties

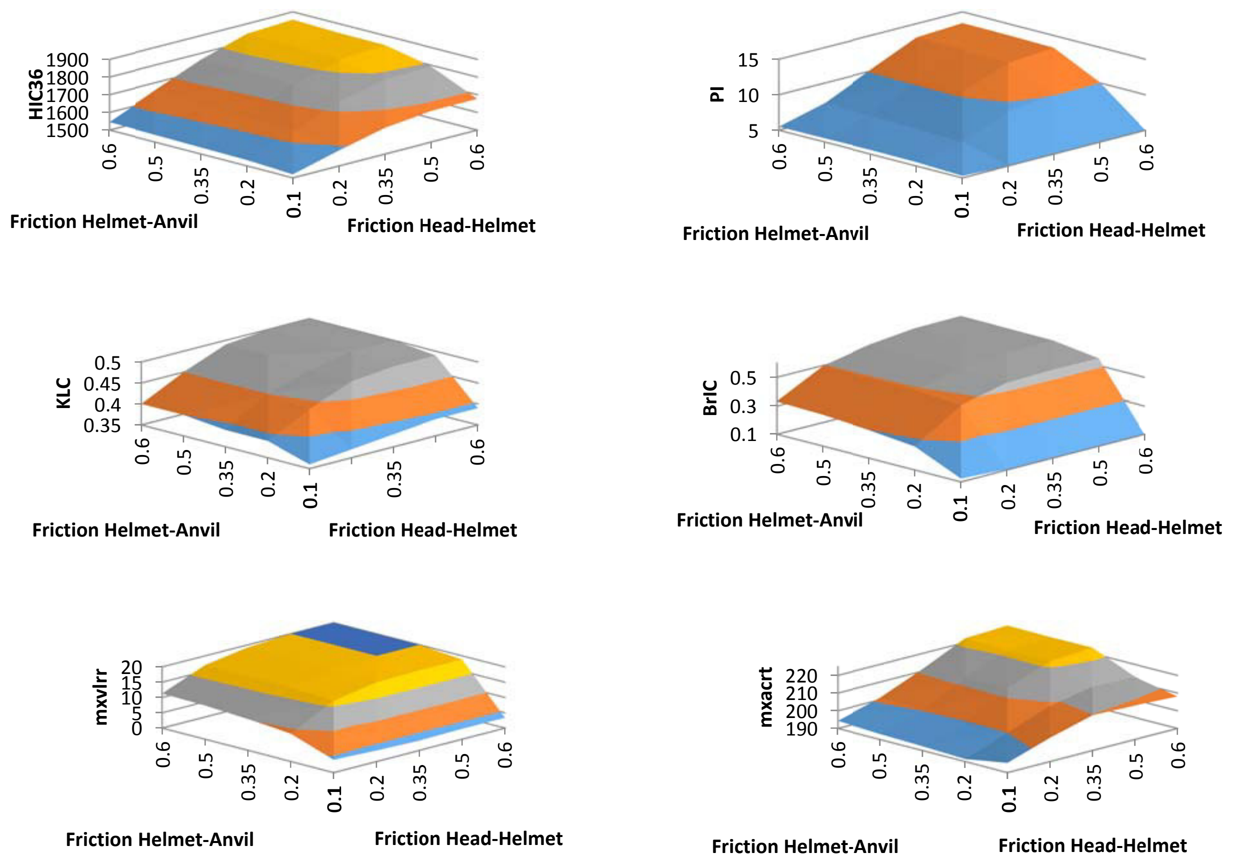

Fig. 23: Effect of friction for HIC36, PI, KLC, BrIC, mxvlrr (res. Rotational velocity), mxacrt (maximum res. translational acceleration)- Pos U

E. Results of numerical study on inertia properties

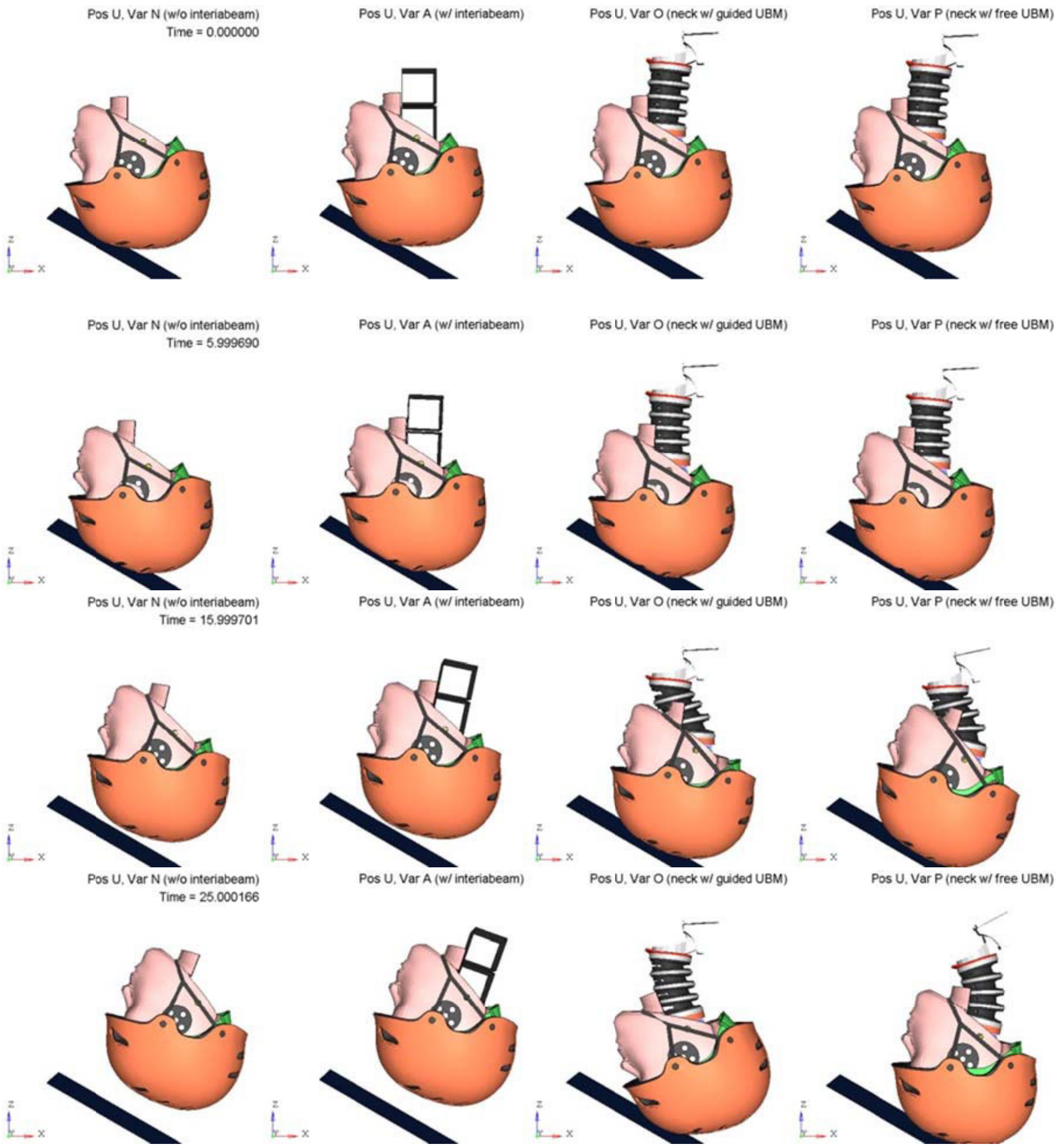

Fig. 24: Effect of neck, upper body mass and interiabeam (Pos U) on kinematics

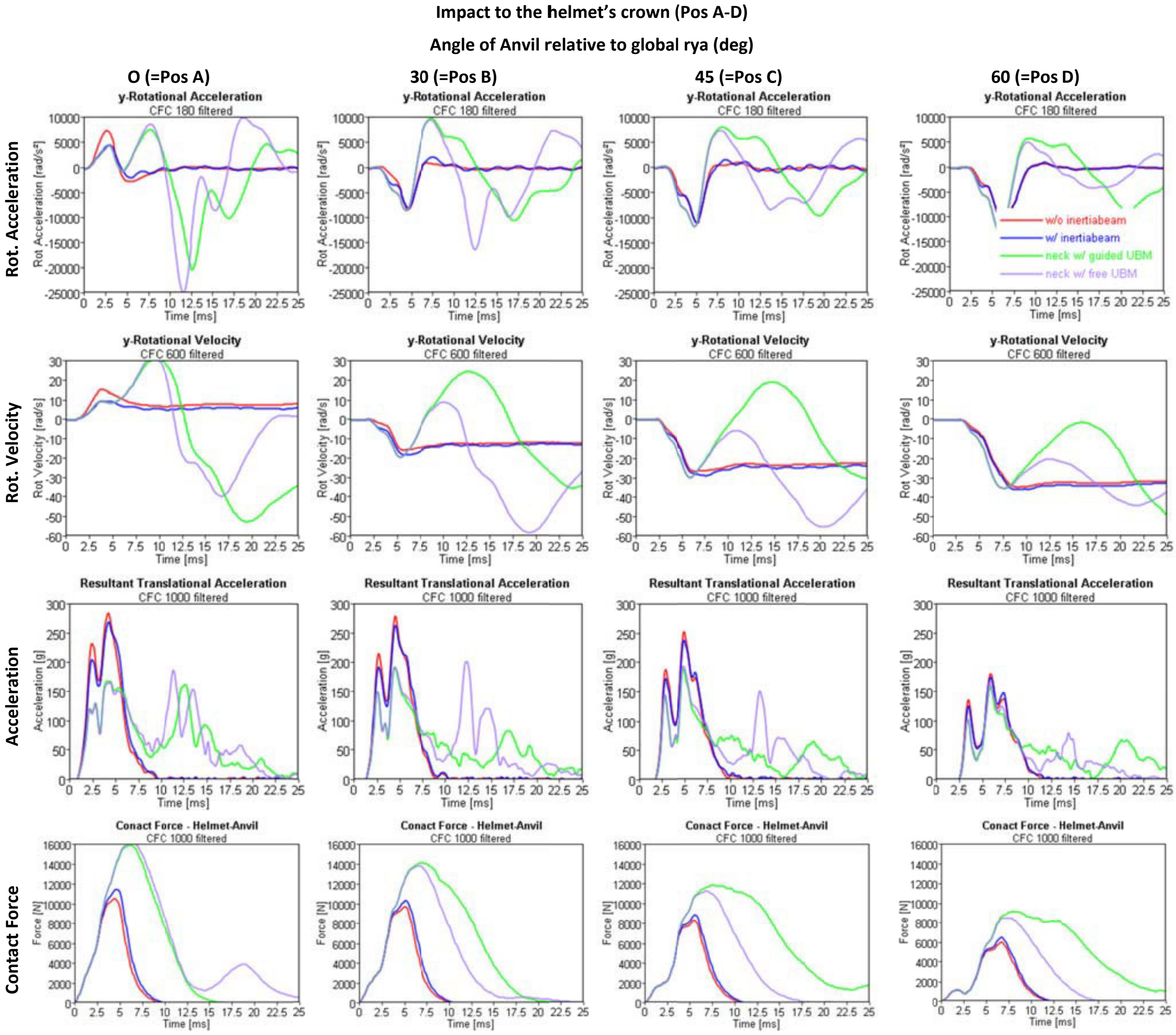

Fig. 25: Effect of neck, upper body mass and interiabeam (impact to the crown) – by anvil angle

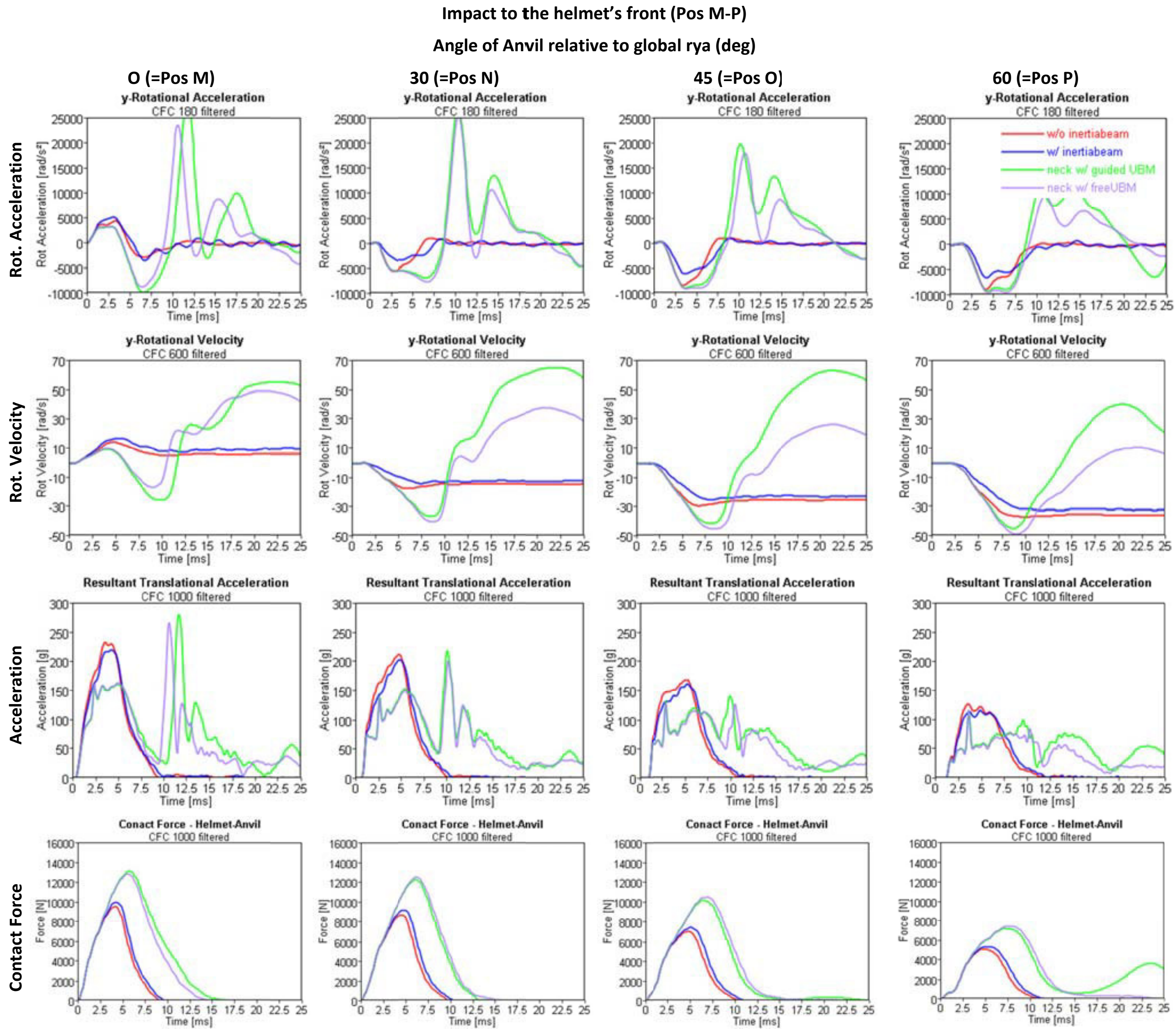

Fig. 26: Effect of neck, upper body mass and interiabeam (impact to the front) – by anvil angle